Strong isotopic effect in the electron-mediated nuclear-nuclear interaction in solids

Frédéric Mentink-Vigier, Laurent Binet,* and Didier Gourier

École Nationale Supérieure de Chimie de Paris (Chimie-ParisTech), Laboratoire de Chimie de la Matière Condensée, UMR-CNRS 7574, 11, rue Pierre et Marie Curie, 75231 Paris Cedex 05, France

(Received 3 January 2011; revised manuscript received 18 March 2011; published 10 June 2011)

We studied the nuclear-nuclear spin interaction mediated by an unpaired electron spin, focusing on an isotopic effect by electron nuclear double resonance (ENDOR) spectroscopy. We investigated a linear cluster Ga-Ti^{3+}-Ga in titanium-doped gallium oxyde $\beta - Ga_2O_3$, whereby the unpaired electron spin density of Ti^{3+} is equally delocalized on the nuclear spins $I = 3/2$ of nearest-neighboring ^{69}Ga and ^{71}Ga nuclei. The linear geometry of the spin arrangement allowed us to easily identify the ENDOR spectra for the three possible isotopic configurations: ^{69}Ga-Ti-^{71}Ga ^{69}Ga-Ti-^{69}Ga and ^{71}Ga-Ti-^{71}Ga. Despite the magnetic moments of ^{71}Ga and ^{69}Ga nuclei differing by only by 27%, the experimental effect of the electron-mediated nuclear-nuclear interaction (pseudodipolar interaction) on the ENDOR spectra is one order of magnitude larger ($\geqslant 1$ MHz) for the symmetrical clusters (^{69}Ga-Ti-^{69}Ga and ^{71}Ga-Ti-^{71}Ga, respectively) than for the asymmetrical cluster ^{69}Ga-Ti-^{71}Ga (<0.1 MHz). This important isotopic effect in the internuclear interaction is a consequence of the cluster symmetry with a local inversion center for the symmetrical configurations, which is lacking in the asymmetrical configuration. These symmetrical clusters thus combine a resolved nuclear-nuclear spin interaction, a nuclear spin monitoring by an unpaired electron, and a large nuclear spin quantum register, which make them attractive for quantum information processing whereby nuclear qubits can be monitored by short selective radiofrequency pulses.

DOI: 10.1103/PhysRevB.83.214409 PACS number(s): 76.70.Dx, 03.67.Lx, 76.30.Fc

I. INTRODUCTION

Internuclear spin-spin interactions are very rarely observed in electron paramagnetic resonance (EPR) spectra of paramagnetic systems. The reason is that dipolar interactions of the order of 1–10 kHz between neighboring nuclei in solids are negligible compared with the width of EPR lines, generally much larger than 10 MHz in solids, and compared with the width of electron nuclear double resonance (ENDOR) lines, generally larger than 100 kHz. The internuclear spin interaction can be enhanced when it is mediated by an unpaired electron spin, the so-called pseudodipolar interaction.[1] However, with a paramagnetic defect or impurity in solids, the resulting interaction remains too small and is generally ignored in EPR and ENDOR spectroscopy. There is a particular situation where this interaction is significantly enhanced, corresponding to two strictly equivalent nuclei interacting via the unpaired electron spin.[1,2] A strong internuclear spin interaction can be observed and resolved in ENDOR spectra if the hyperfine coupling is sufficiently high. This opens the way for the use of coupled nuclear spin systems for quantum information processing, which has been initially proposed for nuclear magnetic resonance (NMR),[3–5] with the advantage that nuclear spins can be monitored and read out with high sensitivity by the unpaired electron spin.[6–11] An important condition for a selective coherent manipulation of individual nuclear spin states is that EPR or ENDOR transitions reflecting these electron-mediated interactions are well separated from each other and from other transitions, implying enhanced nuclear-nuclear spin interaction. Two conditions are thus necessary to find paramagnetic systems exhibiting such an enhanced pseudodipolar interaction. The first is a paramagnetic species interacting with two magnetically equivalent nuclei, and the second is a high electron spin density at each nucleus and thus a predominant contribution of a Fermi contact type to the hyperfine interaction. This requests a delocalized electron wave function made of *s*-type orbitals centered on the nuclei, heavy nuclei to enhance the *s*-type electron spin density at the nucleus, and, as far as inorganic systems are concerned, nuclei from pretransition or posttransition elements.

In this paper, we investigate a spin system made of a pair of gallium nuclei in $\beta-Ga_2O_3$ crystals, which are monitored by the unpaired electron spin of a Ti^{3+} dopant localized in between the two Ga nuclei [Fig. 1(a)]. This is a typical example of a spin bus for quantum information processing as proposed by Mehring and Mende,[9] whereby a set of nuclear spins is monitored by an electron spin. The interest in gallium oxide is that its structure is made of double chains of octahedrally coordinated Ga surrounded by chains of tetrahedral Ga running along the binary **b** axis [Fig. 1(a)]. Undoped $\beta-Ga_2O_3$ is an n-type semiconductor with conduction electron spins inducing a bistable nuclear polarization up to room temperature by the Overhauser effect.[12–14] The bistability manifests itself by a hysteresis of the EPR line with a shape depending on the sweeping mode (up or down) of the magnetic field.[13] This peculiar property is a direct consequence of the linear arrangement of gallium ions, with 4*s* orbitals of octahedral Ga chains forming the conduction band edge.[14] If the ground state of a paramagnetic transition metal impurity in the octahedral site forms a level close to the conduction band edge, we expect an important delocalization of the unpaired electron on gallium nuclei along the octahedral chains. This is the case with Ti^{3+} ions, which exhibit a strong isotropic hyperfine interaction with the nearest Ga neighbors, reaching about 130 MHz.[15] Ti^{3+} in $\beta-Ga_2O_3$ is located on a mirror plane perpendicular to the chains, so that the two crystallographically equivalent nearest neighbor Ga nuclei of the Ti dopant form an ideal cluster for investigating the nuclear-nuclear interaction mediated by an unpaired electron.

Gallium has two isotopes, ^{69}Ga (abundance 60.1%) and ^{71}Ga (abundance 39.9%), both with spin $I = 3/2$. Thus a pair of nuclei separated by a Ti^{3+} ion is described by

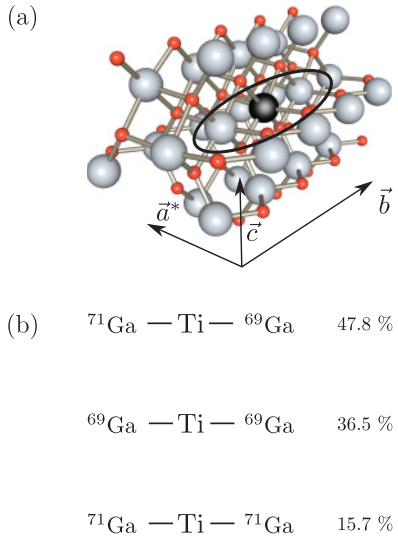

FIG. 1. (Color online) (a) Structure of $\beta-Ga_2O_3$, with the black ellipse highlighting a Ti^{3+} dopant (black sphere) and its two nearest Ga neighbors along the **b** axis. Small spheres are oxygens. (b) The three isotopic configurations of the pairs of nearest Ga neighbors of Ti^{3+} and their relative abundances.

$(2\boldsymbol{I}+1)\times(2I+1)=2^4$ nuclear spin states, and three different isotopic configurations of the system must be considered, as sketched in Fig. 1(b). When both ^{69}Ga and ^{71}Ga isotopes are present in the gallium pair (asymmetrical cluster), the nuclei are magnetically inequivalent. The pseudodipolar interaction is then found to be very weak, and cannot be observed despite the fact that the electron spin density is equally distributed over the two nuclei. When only ^{71}Ga or ^{69}Ga nuclei are present in the cluster, the nuclei are then magnetically equivalent, whatever the magnetic field direction, which considerably enhances the pseudodipolar interaction, leading to well-resolved ENDOR transitions for these symmetrical clusters. This opens the way to selective coherent manipulation of nuclear transitions, as shown by preliminary results by pulsed EPR-ENDOR showing electron and nuclear quantum oscillations in these nuclear spin clusters.[15]

This paper is arranged as follows. The background of the pseudodipolar interaction is briefly described in Sec. II, where it is illustrated by the simple case of an electron spin $S=1/2$ coupled to two equivalent nuclear spins $I=1/2$. Section III describes the preparation method of the β–Ga_2O_3 single crystals and the ENDOR experiment. The detailed analysis of the electron-mediated internuclear spin interaction for asymmetrical and symmetrical gallium clusters is described in Sec. IV. Finally Sec. V deals with a discussion of the results in the context of quantum information processing.

II. THEORETICAL BACKGROUND

The problem of a many-electron system coupled to several nuclei was first studied by Ramsey[16] in 1953. The purpose was to explain small splittings appearing in NMR spectra and specifically in HD spectra. The origin of these small splittings relies on the hyperfine coupling that mixes excited states with the fundamental state in a second-order perturbation treatment. Later on, Feuchtwang[2] (1962) referred to the work of Ramsey in the context of F-center in alkali halides. Feher's model of F-center[17] could not explain the huge number of ENDOR lines of this defect for particular field directions. Here the situation differed from that considered by Ramsey, with only one electron interacting with several nuclei. Contrary to Feher, who considered each nucleus as independent,[17] Feuchtwang developed the full Hamiltonian up to the second order in perturbation, considering the case of several magnetically equivalent nuclei.[2] The effective nuclear spin Hamiltonian presents a term similar to that discussed by Ramsey, representing an indirect interaction between nuclear spins mediated by the unpaired electron. The theory was successfully applied to the F-center in KCl.[2] In 1968, Schoemaker[1] revisited and modified Feuchtwang's model. Discussing more precisely the comparison between the second order hyperfine interaction $\mathbf{H}^{(2)}_{h.f.}$ and the quadrupolar interaction $\mathbf{H}_Q$, Schoemaker slightly changed the formalism and distinguished two clear-cut cases, $\mathbf{H}^{(2)}_{h.f.}\gg\mathbf{H}_Q$ and $\mathbf{H}^{(2)}_{h.f.}\ll\mathbf{H}_Q$. He named the above mentioned internuclei interaction pseudodipolar, since it appears as a dipolar-type nucleus-nucleus interaction mediated by an unpaired electron. The theory was successfully applied to the EPR spectrum of the I_2^- center in (KCl:KI:Pb^{2+}).[1] This approach was next applied to the ^{27}Al-ENDOR study of F^+ center in β-alumina[18] and to the ENDOR of the Ga vacancy in GaP.[19]

In the most general case, when applying a magnetic field $\mathbf{B_0}$ to an electron interacting with N nuclei, the general form of the Hamiltonian is given by

$$H=\beta\mathbf{S}\cdot\mathbf{g}\cdot\mathbf{B_0}+\sum_{i\leqslant N}(\mathbf{S}\cdot\mathbf{A}_i\mathbf{I}_i+\mathbf{I}_i\cdot\mathbf{Q}_i\cdot\mathbf{I}_i-g_{n,i}\beta_n\mathbf{I}_i\cdot\mathbf{B_0}), \quad (1)$$

where the terms in the sum over all nuclei correspond to the hyperfine, quadrupolar, and nuclear Zeeman interactions, respectively. The so-called pseudodipolar interaction arises when deriving an effective nuclear Hamiltonian from Eq. (1) with a Pryce perturbation development[20] up to the second order (see appendix). In the case of two magnetically inequivalent nuclei characterized by two isotropic hyperfine interaction constants A_1 and A_2, the pseudodipolar term can be written simply as[1,2,18]

$$\mathbf{H}_{p.\mathrm{dip.}}(m_s)=m_s\frac{A_1A_2}{2g\beta B_0}[\mathbf{I}_1^+\mathbf{I}_2^-+\mathbf{I}_1^-\mathbf{I}_2^+], \quad (2)$$

which corresponds to a "flip-flop" term between the two nuclei. We expect an isotopic effect in the case of the Ga-Ti-Ga spin system in $\beta-Ga_2O_3$: Ti, with two clear-cut situations corresponding to the symmetrical clusters (i.e., ^{71}Ga-Ti-^{71}Ga and ^{69}Ga-Ti-^{69}Ga) and asymmetrical clusters ^{69}Ga-Ti-^{71}Ga. To illustrate this isotropic effect, let us consider the simplified model of a linear trimer $I-S-I$ composed of two nuclei $I=1/2$ separated by a paramagnetic species with $S=1/2$. In addition, the nuclei possess two isotopes I_1 and I_2 with the respective nuclear Larmor frequencies ν_1 and ν_2, and Fermi contact-type hyperfine interaction A_1 and A_2 such as $A_1/A_2=\nu_1/\nu_2$. If we neglect the interaction between the two nuclear spins, we may consider the system as the sum of two independent systems, respectively I_1-S and $S-I_2$ dimers. In the case $A_i/2>\nu_i>0$, the two $m_s=\pm1/2$ ENDOR

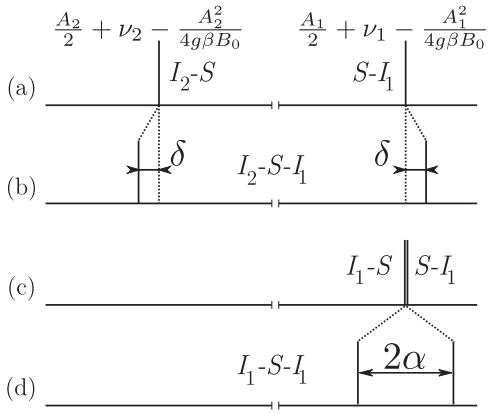

FIG. 2. Schematic representation of the $m_s = -1/2$ ENDOR lines for the case of an $S = 1/2$ electron coupled to two nuclei $I_1 = I_2 = 1/2$, with Larmor frequencies ν_1 and ν_2, and isotropic hyperfine interactions $A_i > \nu_i > 0$ $(i = 1,2)$. Cases (a) and (b) correspond to an asymmetrical cluster I_1–S–I_2 without (a) and with (b) the pseudodipolar interaction. Case (a) corresponds to two independent S–I_1 and S–I_2 systems. Cases (c) and (d) correspond to a symmetrical cluster I_1–S–I_1 without (c) and with (d) the pseudodipolar interaction. Case (c) corresponds to two independent S–I_1 systems.

frequencies up to second order in the hyperfine interaction are $A_1/2 \pm \nu_1 \mp /A_1^2/4g\beta B_0$ and $A_2/2 \pm \nu_2 \mp A_2^2/4g\beta B_0$ for I_1-S and $S-I_2$ systems, respectively [Fig. 2(a)]. It is important to note that when both nuclei are considered together in a single system, each ENDOR transition of nucleus i corresponding to $\Delta m_i = \pm 1$ and $\Delta m_j = 0$ $(\{i,j\} = \{1,2\})$ is degenerate owing to the $2I_j + 1$ possible values for the spin quantum number m_j of the other nucleus j. Including the pseudodipolar interaction in the asymmetrical isotope configuration, i.e., considering the electron mediated coupling between nuclei in the system $I_2 - S - I_1$, slightly changes the ENDOR spectrum.

As discussed in the appendix, in the case where $I_1 = I_2 = 1/2$, the pseudodipolar interaction leads to a shift of the ENDOR lines by [Fig. 2(b)]

$$\delta \approx \left(\frac{A_1 A_2}{2g\beta B_0}\right)^2 \frac{m_s}{A_1 - A_2} \tag{3}$$

but does not lift the twofold degeneracy of the ENDOR lines. The case of the symmetrical isotope configuration I_1-S-I_1 is shown in Figs. 2(c) and 2(d). Without interactions between nuclei, the two ENDOR lines of the independent systems I_1-S are superimposed. The pseudodipolar interaction between I_1 nuclei produces a splitting 2α of the two lines given by

$$2\alpha = \frac{m_s A_1^2}{g\beta B_0}. \tag{4}$$

The difference between the two situations appears clearly in Eqs. (3) and (4). The pseudodipolar interaction acts as a third-order effect of the hyperfine interaction with respect to the electron Zeeman term in the spin Hamiltonian for the asymmetrical isotope configuration, while it is a second-order effect for the symmetrical one. The relative orders of magnitude of the effects of the pseudodipolar interaction in the asymmetrical and symmetrical clusters are given by $\delta/2\alpha = A_2^2/4g\beta B_0(A_1 - A_2) \approx 10^{-2}$, with $A_1 = 128$ MHz, $A_2 = 100$ MHz, and $g\beta B_0 \approx 9500$ MHz, corresponding to the parameters of $\beta - Ga_2O_3$.[15] This points to a strong isotopic effect enhancing the pseudodipolar interaction in the case of the symmetrical cluster.

III. MATERIAL AND METHODS

Single crystals of $\beta-Ga_2O_3$ doped with TiO_2 were grown by the floating zone method.[21] The powder of $\beta-Ga_2O_3$ (Alpha Aesar, 99.99%) and 1 wt% of TiO_2 (Sigma Aldrich, 99.9%) were mixed and pressed, and the resulting bar was sintered at 1000 °C. The crystal was grown from the sintered bar and starting from an undoped seed of $\beta-Ga_2O_3$ obtained from a previous synthesis. The seed was aligned such as the crystal grows along the **b** axis. The resulting crystal is transparent and slightly red. The ratio Ti/Ga $\approx$ 0.003 was measured by inductively coupled plasma mass spectroscopy (ICP-MS) analysis at *Service Central d'Analyse* of CNRS, Solaize, France.

A UV-visible absorption spectrum, performed on a Varian Cary 6000i spectrometer, exhibited a broadband at about 518 nm (results not shown), consistent with the $^2T_2 \rightarrow {}^2E$ transition of Ti^{3+} in an octahedral environment. The crystals were studied by cw-EPR and cw-ENDOR spectroscopy at 20−30 K with an X-band (9.4 GHz) Bruker Elexsys E500 spectrometer using a 4122SHQ/0111 cavity and a TM_{110} cavity for EPR and ENDOR, respectively. The radiofrequency (rf) field was amplified by a 500A100A broadband Amplifier Research amplifier. A 25-kHz frequency modulation of the rf carrier, with modulation depth 100 kHz was used for the detection. With this modulation scheme, the ENDOR signal takes the form of the first derivative of the ENDOR enhancement.

The ENDOR spectra were simulated for $\mathbf{B_0} \parallel \mathbf{c}$ using the spin Hamiltonian parameters determined in a previous work[15] and given in Table I.

The spectra were calculated either by diagonalization of the full Hamiltonian or by second-order perturbation theory. The diagonalization was performed with the *EasySpin* software package[22] by using the complete set of tensors. The line intensities were obtained taking into account Fermi's golden rule, Boltzmann's population, and the abundance

TABLE I. Principal values in MHz and Euler angles relative to the (**c**, **a***, **b**) frame of the hyperfine (**A**) and quadrupolar (**Q**) tensors used for the diagonalization of the spin Hamiltonian

	A_x	A_y	A_z	$(\alpha_A,\beta_A,\gamma_A)$	Q_x	Q_y	Q_z	$(\alpha_Q,\beta_Q,\gamma_Q)$
^{71}Ga	128.1	126.6	132.9	(0,0,0)	−0.76	−0.06	0.82	(0,90,0)
^{69}Ga	100.8	99.6	104.6	(0,0,0)	−1.20	−0.10	1.30	(0,90,0)

of a given isotopic configuration. This procedure gives a good description of the ENDOR spectrum. The physical meaning of the different transitions was analyzed by using the perturbation method. The latter was implemented with two in-house programs running on Octave/Matlab. The formulas were adapted from Iwasaki's paper[23] for the asymmetrical cluster, and from Schoemaker's paper[1] for the symmetrical clusters. The expressions are given in the appendix. To simplify the simulations with the perturbation method, we considered isotropic hyperfine and axial quadrupolar interactions. The isotropic hyperfine coupling approximation is justified since, in the case of first-neighbor gallium nuclei considered in the clusters, the anisotropic part contributes only about 1.5% of the whole hyperfine interaction. The axial quadrupolar interaction approximation is quite strong, since the asymmetry parameter is actually $\eta = 0.85$.[15] These approximations gave the right pattern for the ENDOR spectrum, but the peak positions differed somewhat between perturbation calculation and experimental data. This discrepancy is due to the axial approximation in the quadrupolar interaction. As the perturbation approach was used to analyze only the physical meaning of the nuclear interactions within the clusters but not to extract exact parameters, we used effective values for the second-order hyperfine coupling $(A^2/2g\beta B_0)_{eff} = 0.75 \times A^2/2g\beta B_0$ and for the quadrupolar interaction $Q_{eff} = 1.6 \times Q$ to adjust ENDOR line positions obtained from perturbation calculations to experimental values.

IV. RESULTS

A. General features of EPR and ENDOR

The EPR spectrum at 20 K of a single crystal of $\beta-Ga_2O_3$ doped with 0.3% of Ti^{3+} is shown in Fig. 3(a) for the external field orientation $\mathbf{B_0} \parallel \mathbf{c}$. The arrow indicates the magnetic field setting used for the ENDOR experiment. The EPR spectrum reveals a partially resolved hyperfine interaction with nearest-neighbor ^{71}Ga and ^{69}Ga nuclei. For this orientation the hyperfine interactions measured by ENDOR are $^{71}A = 128.1$ MHz and $^{69}A = 100.8$ MHz, respectively, and the electron spin density obtained from the isotropic part of the hyperfine interaction is $\rho_{4s} = 0.017$ in the 4s atomic orbital of each gallium ion.[15] The EPR spectrum is the sum of three isotope configurations spectra ^{69}Ga-Ti-^{71}Ga (47.8%), ^{69}Ga-Ti-^{69}Ga (36.5%) and ^{71}Ga-Ti-^{71}Ga (15.7%). According to the EPR selection rule, $\Delta m_s = \pm 1$, $\Delta^x m = 0$ ($x = 71$ or 69), and $\Delta M = 0$ (M is the total z component of the two nuclear spins); the theoretical EPR transitions are shown as stick diagrams in Fig. 3(b). By setting the magnetic field in the middle of the EPR spectrum for the ENDOR experiment [Fig. 3(a)], one selects the hyperfine transitions $M = 0$ for the symmetrical clusters ^{71}Ga-Ti-^{71}Ga and ^{69}Ga-Ti-^{69}Ga, and the hyperfine transitions $^{71}m = \pm 1/2$ and $^{69}m = \pm 1/2$ for the asymmetrical cluster ^{69}Ga-Ti-^{71}Ga.

Considering the ENDOR transitions $\Delta m_s = 0$, $\Delta^x m = \pm 1$ and a first-order treatment of the hyperfine and quadrupolar interactions, we expect six ENDOR lines for each isotope, at frequencies

$$^xA/2 \pm^x \nu_n \mp 3^x m_q \times^x Q. \quad (5)$$

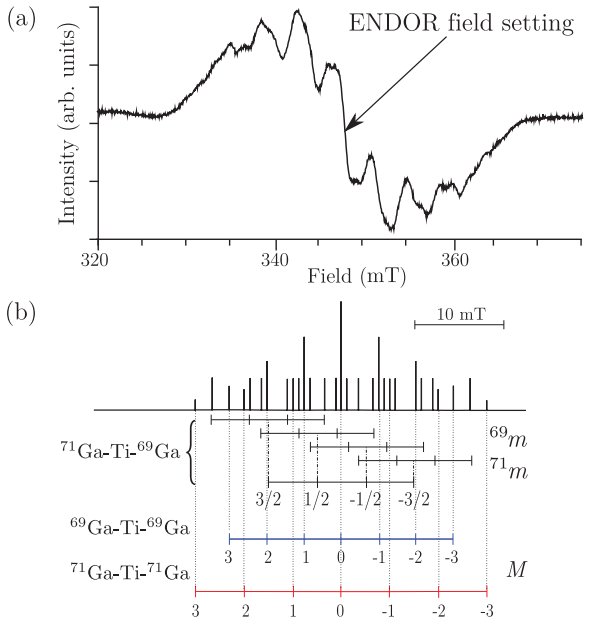

FIG. 3. (Color online) (a) cw-EPR spectrum of Ti^{3+} at 30 K in $\beta - Ga_2O_3$: Ti for $\mathbf{B_0} \parallel \mathbf{c}$. The arrow indicates the field setting for ENDOR experiments. (b) Stick diagram of the EPR spectrum taking into account the first-neighbor Ga nuclei.

where $^xm_q = (^xm' + ^x m)/2$, where $^xm'$ and ^xm are the nuclear quantum numbers between which the transition takes place, and ^xQ the effective value of the quadrupolar interaction along the magnetic field direction for isotope $x = 69$ or 71. The high frequency part (35–78 MHz) of the ENDOR spectrum shown in Figs. 4(a) and 4(b), corresponds to the first-neighbor ^{71}Ga and ^{69}Ga nuclei. Other neighbors give transitions at lower frequencies.[15] In Figs. 4(a) and 4(b), the top stick spectra are the theoretical ENDOR spectra for the asymmetrical ^{69}Ga-Ti-^{71}Ga cluster and the bottom stick spectra correspond to the symmetrical ^{69}Ga-Ti-^{69}Ga and ^{71}Ga-Ti-^{71}Ga clusters. In Fig. 4(a) stick spectra are calculated using diagonalization of the spin Hamiltonian, Eq. (1). In Fig. 4(b), stick spectra are calculated using perturbation theory, including only the diagonal terms of the hyperfine interaction within each electron spin manifold [see Eqs. (A8)–(A10) and (A14)–(A16) in the appendix for the asymmetrical and symmetrical clusters, respectively]. The ENDOR transitions in this stick spectrum are labeled by their m_s and m_q values.

B. Asymmetrical clusters ^{69}Ga-Ti-^{71}Ga

The most intense ENDOR lines in Fig. 4 originate from the hyperfine interaction with the Ga neighbors of Ti^{3+} in the asymmetrical clusters ^{69}Ga-Ti-^{71}Ga. As expected for this cluster, each nucleus yields six ENDOR lines. This result is verified both by diagonalizing the full Hamiltonian with the two nuclei ^{69}Ga and ^{71}Ga [Eq. (1)] and using perturbation theory. This is shown by the theoretical stick spectra at the top of Figs. 4(a) and 4(b), which accurately fit with the experimental spectrum. However, the theoretical stick spectrum obtained from the diagonalization of the spin Hamiltonian of the cluster shows that each ENDOR line is actually split into up to four sublines, as shown in the inserts

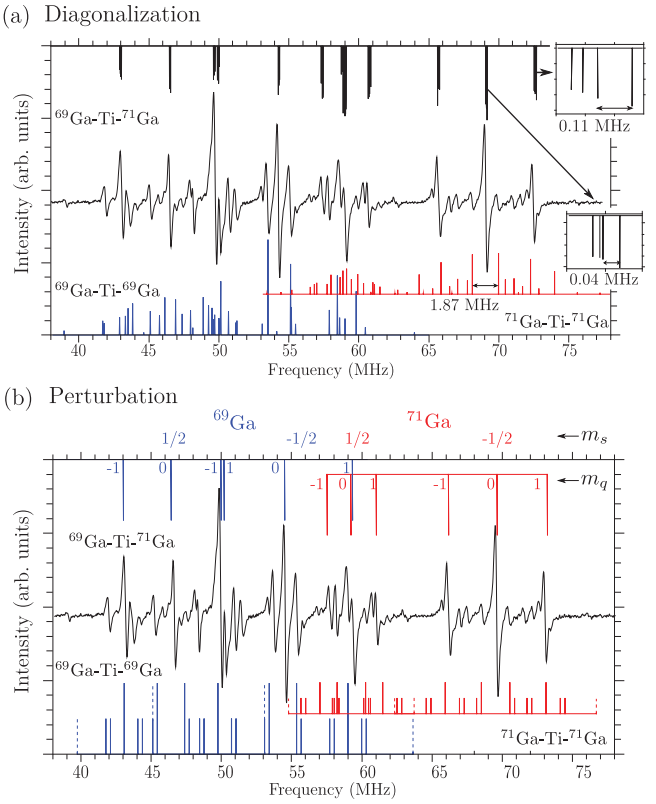

FIG. 4. (Color online) High-frequency part of the experimental ENDOR spectrum of $\beta-Ga_2O_3$: Ti^{3+} at 20 K for $\mathbf{B_0} \parallel \mathbf{c}$, compared with spectra calculated (a) by diagonalization of the full spin Hamiltonian, and (b) by second-order perturbation. The theoretical stick spectra of ^{69}Ga-Ti-^{71}Ga are displayed at the top of (a) and (b), and the theoretical stick spectra of ^{69}Ga-Ti-^{69}Ga and ^{71}Ga-Ti-^{71}Ga are displayed at the bottoms. The insets in (a) represent a zoom on peaks at ≈ 72.5 MHz ($m_s = -1/2, m_q = (m'_I + m_I)/2 = 1$) and at 69 MHz ($m_s = -1/2$, $m_q = 0$). The stick spectra obtained by second-order perturbation theory in (b) correspond to $\Delta m_1 = \pm 1$, $\Delta m_2 = 0$, or $\Delta m_1 = 0$, $\Delta m_2 = \pm 1$ transitions (full lines), and to transitions $\Delta M = \pm 1$ with $\Delta m_1 = \pm 1$, $\Delta m_2 = \mp 2$ or $\Delta m_1 = \mp 2$, $\Delta m_2 = \pm 1$ (dashed lines).

in Fig. 4(a) for the ENDOR peak $m_s = -1/2$, $^{71}m_q = 1$ [with $^{71}m_q = (^{71}m' + ^{71}m)/2$] and $m_s = -1/2$, $^{71}m_q = 0$ for the ^{71}Ga nucleus. This splitting appears only when both nuclei in the cluster are included in the spin Hamiltonian but not when the nuclei are considered separately. This shows that this splitting is due to an indirect interaction between the two nuclei in the cluster. As discussed in the appendix, in the case where I_1 and/or $I_2 > 1/2$, the pseudodipolar interaction should induce a small splitting of each ENDOR line $m_i \leftrightarrow m_i + 1$ by

$$2m_s \left(\frac{A_i A_j}{2g\beta B_0}\right)^2 \frac{I_j(I_j+1) - m_j^2 + 2m_i m_j + m_j}{A_i - A_j}, \qquad (6)$$

with $\{i,j\} = \{1,2\}$, when the nondiagonal terms due to the pseudodipolar interaction are included in the calculation. With $A_1 = 128.1$ MHz for ^{71}Ga, $A_2 = 100.8$ MHz for ^{69}Ga and $I_1 = I_2 = 3/2$, we thus predict splittings of about 0.03 MHz and 0.08 MHz for the $-1/2 \leftrightarrow 1/2$ and $\pm 1/2 \leftrightarrow \pm 3/2$ transitions on ^{71}Ga, respectively. These values are of the same order of magnitude as those obtained from the diagonalization

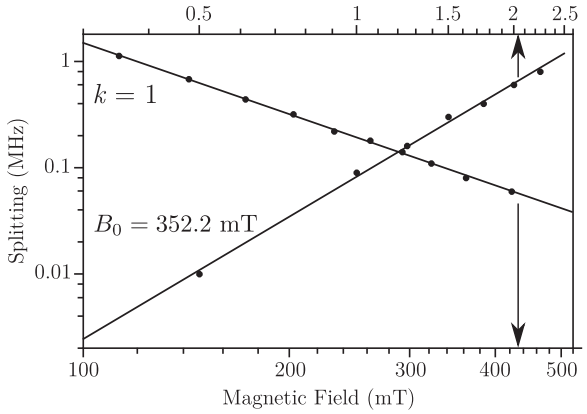

FIG. 5. Theoretical variations of the splitting of the $m_s = -1/2$, $m_q = 1$ transition of the first-neighbor ^{71}Ga nucleus; versus the external magnetic field amplitude B_0 at fixed hyperfine interaction ($k = 1$) and versus the hyperfine interaction (versus k) at fixed B_0. Calculations are made by diagonalization of the exact Hamiltonian.

of the spin Hamiltonian as shown in the insets in Fig. 4(a). This shows that the pseudodipolar interaction between the two nuclei in the cluster significantly contributes to the splitting of the ENDOR lines of the asymmetrical clusters. However, as discussed in the appendix, the pseudodipolar interaction should split the ENDOR lines into at most three sublines, while the diagonalization yields a splitting into four sublines. This is certainly due to other third-order contributions with respect to the electron Zeeman Hamiltonian, which are not taken into account in the effective nuclear Hamiltonian derived from a second-order development.

To confirm that the small (experimentally unresolved) splittings of the ENDOR lines result from third-order effects, we monitored the dependence on the magnetic field B_0 and the dependence on the hyperfine coupling constant A of the largest splitting of the ^{71}Ga-ENDOR line in the inset of Fig. 4(a), computed by diagonalization. To study the dependence on A, the hyperfine coupling constant for ^{71}Ga and ^{69}Ga were varied by changing a scaling factor k such that $A = kA_{\text{exp}}$ with $A_{\text{exp}} = 128.1$ MHz for ^{71}Ga and $A_{\text{exp}} = 100.8$ MHz for ^{69}Ga. The result of the calculation is shown in Fig. 5, which represents the log of the splitting versus k for $B_0 = 352.2$ mT and versus B_0 for $k = 1$. Linear simulations of the results give slopes -2.22 ± 0.02 and 2.97 ± 0.02, respectively. It thus appears that the splittings scale with A and B_0 as $\sim A^3/(g\beta B_0)^2$, which means that they result from a third-order effect and reach at most ~ 0.1 MHz for Ga nuclei in asymmetrical clusters.

C. Symmetrical clusters: ^{71}Ga-Ti-^{71}Ga and ^{69}Ga-Ti-^{69}Ga

In addition to the intense ENDOR lines of ^{69}Ga and ^{71}Ga in asymmetrical clusters, the experimental spectrum in Fig. 4 shows a lot of weaker lines that cannot be accounted for by considering only the asymmetrical cluster ^{69}Ga-Ti-^{71}Ga. These additional lines do not arise from some Ti^{3+} perturbed by neighboring defects, since they follow the same angular variations as the main lines.[15] As anticipated, they are due to transitions of ^{69,71}Ga in the symmetrical clusters ^{69}Ga-Ti-^{69}Ga and ^{71}Ga-Ti-^{71}Ga. This is demonstrated by the diagonalization

of the Hamiltonian Eq. (1) for these configurations, with the same hyperfine and quadrupolar parameters as for the asymmetrical cluster. The corresponding ENDOR theoretical stick spectra are shown of the bottom of Fig. 4(a). The calculated line positions are in good agreement with the experimental ones. However, the line intensities, computed from Fermi's golden rule and Boltzmann populations,[22] do not accurately match the experimental values. The reason is that ENDOR intensities also strongly depend on the relaxation rates of the spin system (Ref. 24, p. 171). Contrary to the situation of an asymmetrical cluster for which the pseudodipolar interaction is a third-order perturbational effect, this interaction is now a second-order effect for the symmetrical clusters. This is shown by computing the ENDOR lines with the perturbation method up to second-order, with the corresponding stick spectra shown at the bottom of Fig. 4(b). Although diagonalization and perturbation methods give different spectra, their general features are similar.

The origin of the multiple line ENDOR spectra for symmetrical clusters can be understood by considering the high-frequency part ($m_s = -1/2$) of the ^{71}Ga-ENDOR spectrum between 60 and 80 MHz. Figure 6(a) shows the nuclear spin energy levels in the electron $m_s = -1/2$ manifold calculated with the perturbation method for the symmetrical ^{71}Ga-Ti-^{71}Ga cluster. The details of the calculation are developed in the appendix. The different contributions to the nuclear Hamiltonian, namely $\mathbf{H}^{(1)}_{h.f.}$, $\mathbf{H}_{n.z.}$, $\mathbf{H}_{p.\mathrm{dip}}$, $\mathbf{H}^{(2)}_{h.f.}$ and $\mathbf{H}^{(1)}_{Q}$ are the first-order hyperfine interaction, the nuclear Zeeman interaction, the pseudodipolar interaction, the remaining second-order hyperfine interaction, and the first-order quadrupolar interaction, respectively. For graphical reasons, the effects of $\mathbf{H}_{n.z.}$, $\mathbf{H}^{(2)}_{h.f.}$, $\mathbf{H}^{(1)}_{Q}$, and $\mathbf{H}_{p.\mathrm{dip}}$ are amplified by a factor of 2 with respect to $\mathbf{H}^{(1)}_{h.f.}$. The kets on the right-hand part of the diagram represent the $|m_1,m_2,\pm\rangle$ nuclear spin states, where m_1 and m_2 are the components along the magnetic field of the gallium nuclear spins I_1 and I_2 in the cluster, and $M = m_1 + m_2$. The + and − signs represent the parity, $\mathcal{P}$, of the spin state (see the appendix for details). $\mathcal{P}$ is a good quantum number in symmetrical pairs because the strict equivalence of the two nuclei in these configurations implies that the nuclear eigenstates are either symmetrical or antisymmetrical with respect to the interchange of nuclei. Starting from the first-order hyperfine interaction $\mathbf{H}^{(1)}_{h.f.}$, which splits the $(2I+1)(2I+1) = 16$-fold degeneracy of the m_s state into seven equidistant hyperfine levels characterized by $M = (m_1 + m_2) = \pm3, \pm2, \pm1, 0$, the effect of $\mathbf{H}_{n.z.}$, $\mathbf{H}^{(2)}_{h.f.}$ (excluding the pseudodipolar interaction), and $\mathbf{H}^{(1)}_{Q}$ is to shift the M levels and to lift the degeneracy of the $M = 0, \pm1$ levels of ^{71}Ga-Ti-^{71}Ga. The pseudodipolar interaction $\mathbf{H}_{p.\mathrm{dip}}$ lifts the remaining degeneracy of the levels characterized by $m_1 = m_2 \pm 1$ and opposite parity, which correspond to the $M = \pm2$ and 0 levels.

ENDOR transitions obey the selection rules $\Delta M = \pm1$, (with $\Delta m_1 = \pm1$, $\Delta m_2 = 0$, or $\Delta m_1 = 0$, $\Delta m_2 = \pm1$) and $\Delta\mathcal{P} = 0$, which yield 18 transitions (full and dotted lines in Fig. 6). Taking into account partially allowed transitions characterized by $\Delta M = \pm1$ with $\Delta m_1 = \pm1$, $\Delta m_2 = \mp2$ or $\Delta m_1 = \mp2$, $\Delta m_2 = \pm1$ (lines 9 and 11 in Fig. 6), 20 ENDOR transitions[2] are expected in each m_s manifold (stick spectrum

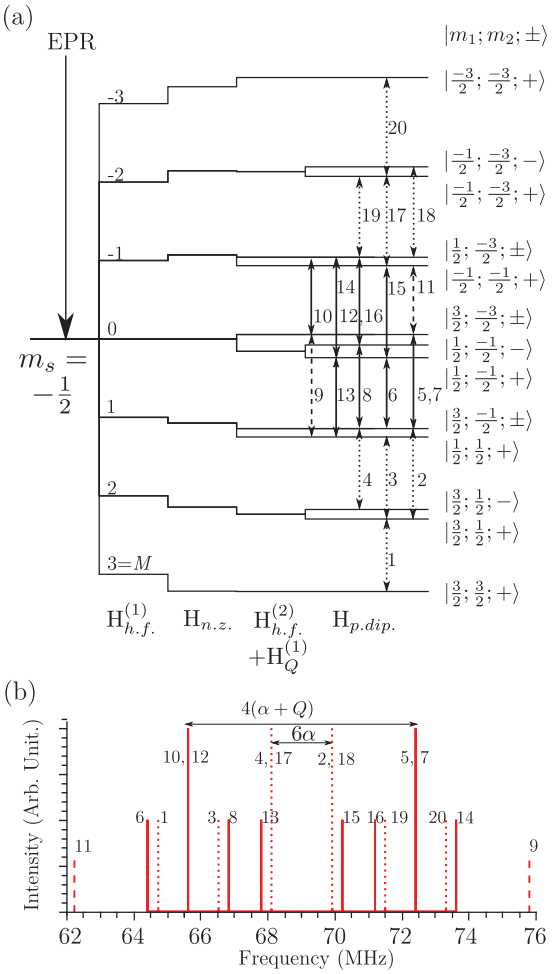

FIG. 6. (Color online) (a) Nuclear spin energy level diagram in the $m_s = -1/2$ electron spin manifold for the symmetrical cluster ^{71}Ga-Ti-^{71}Ga calculated by second-order perturbation theory when $\mathbf{B_0} \parallel \mathbf{c}$. (b) Corresponding ENDOR spectrum. Full and dotted arrows/lines represent allowed transitions ($\Delta m_i = \pm1, \Delta m_j = 0$, $\{i,j\} = \{1,2\}$) and dashed arrows/lines represent partially allowed transitions ($\Delta m_i = \pm1, \Delta m_j = \mp2$, $\{i,j\} = \{1,2\}$). Full arrows/lines represent transitions obtained by saturating the EPR transition corresponding to $m_1 + m_2 = 0$, exclusively.

of Fig. 6. For a single symmetrical cluster, this yields a total of 40 ENDOR transitions. In principle, considering the standard ENDOR mechanism in solids,[25] the most intense ENDOR lines result from the relaxation process $\Delta(m_s + M) = 0$ (flip-flop mechanism). Thus, keeping in mind that the field setting used for our ENDOR experiment correspond to the $M = 0$ EPR transition of the symmetrical clusters, we expect ENDOR lines only between $M = \pm1$ and $M = 0$ hyperfine levels, which correspond to transitions 5–16 in Fig. 6. However, the comparison of the stick and experimental spectra of Fig. 4 shows that at least transitions 2–4 and 17–19 also occur, corresponding to transitions between $M = \pm2$ and $M = \pm1$ levels (dotted lines in Fig. 6). The reason is that the relaxation mechanism is more complex than a simple "flip-flop" process. For example, the fact that the hyperfine interaction has a small anisotropic contribution also favors a

relaxation mechanism of the type $\Delta(m_s + M) = \pm 2$ (flip-flip mechanism: Ref. 26 chap. 4).

The pseudodipolar interaction induces a drastic change in the ENDOR spectrum of symmetrical clusters as compared with asymmetrical ones. The spectral effect of the pseudodipolar interaction can be assessed from the separation of the two ENDOR lines of the symmetrical cluster corresponding to transitions 4–17 and 2–18 in Fig. 6 and flanking the central line $m_q = 0$ of the asymmetrical clusters. As shown in Fig. 4(a) in the case of the symmetrical cluster ^{71}Ga-Ti-^{71}Ga, this separation is about 1.87 MHz. Thus the pseudodipolar interaction has a measurable effect exceeding 1 MHz on the ENDOR spectra of the symmetrical clusters, while this effect is weak (<0.1 MHz) and experimentally unresolved in the case of the asymmetrical cluster, though the two gallium nuclei are crystallographically equivalent in both types of clusters. This puts forward a strong isotopic effect on the electron-mediated indirect nucleus-nucleus interaction.

V. DISCUSSION

Nuclear spins have long been considered as attractive systems to implement quantum information processing owing to the long nuclear spin coherence times and the possibility of coherent control with rf pulses.[3–5] Up to now, most developments of quantum processing based on NMR were achieved in the liquid state at room temperature with molecules bearing nuclear spins $I = 1/2$ only and despite successfull demonstrations of quantum algorithms,[4] NMR-based quantum processing suffers from major limitations. First, the very low thermal nuclear spin polarization and the use of pseudopure states for quantum computation makes the scaling up of spin-based quantum processors very difficult.[27–29] Second, in the liquid state, all traceless interactions are averaged out, leaving only the weak scalar J coupling with $J \approx 10-100$ Hz to perform multiqubit gates, thus limiting both the gate speed, which scales as the interspin interaction, and the size of the spin system owing to the fast decrease of J with internuclear spacing.[5] Several approaches have been proposed to circumvent these obstacles. The number of qubits can be increased without increasing the number of nuclei by using nuclear spins $I > 1/2$ since it was shown in this case that either the whole set or a subset of the spin states can be mapped onto a multiqubit system.[30–33] It was also proposed to consider paramagnetic systems whereby nuclear spins are monitored by an unpaired electron spin for preparation and readout.[6–11] Such systems would benefit from the high electron-to-nuclear gyromagnetic ratio $\gamma_e/\gamma_n \approx 10^3$ so that in the preparation step, the transfer of the electron spin polarization to the nuclei would increase the nuclear spin polarization by this factor of 10^3, and in the readout step the transfer of the computation results back to the electron spin would enhance the sensitivity of detection by another factor of 10^3. A third approach consists of using other nuclear interactions, which can be much stronger than the J coupling to perform faster multiqubit gates. For instance, computational schemes based on the dipolar interaction $D \approx 10$ kHz in liquid crystals[34] or on the quadrupolar interaction $P \approx 1$ MHz in liquid crystals[31,32] or in solids[33] were proposed, though in these proposals the actual quadrupolar interaction was reduced to effective values of about 10^3-10^4 Hz due to low ordering of the liquid crystals or to magic-angle spinning. Another interaction between nuclei is the indirect pseudodipolar interaction studied in this work. It is mediated by an unpaired electron spin, and thus occurs specifically in paramagnetic systems where two or more nuclei simultaneously interact with a same unpaired electron via the hyperfine interaction.

The spin system investigated in this work combines altogether the approaches mentioned above to overcome the limitations of NMR-based quantum processing, namely nuclear spins with $I > 1/2$, nuclear monitoring by an electron spin and a strong pseudodipolar interaction between nuclei. When the nuclei are inequivalent i.e., characterized by different hyperfine coupling constants, the pseudodipolar interaction is very weak and, as shown in Sec. IV, is only a third-order effect in the electron-nuclei spin Hamiltonian. However, when the nuclei are magnetically equivalent, the pseudodipolar interaction occurs as a second-order effect and scales as A^2/Δ, where Δ is the electron Zeeman energy. In strongly coupled electron-nuclei systems where $A \approx 100$ MHz and with $\Delta \approx 10^4$ MHz at typical magnetic fields $B_0 \approx 0.3$ T used in EPR, the pseudodipolar interaction can then reach a quite high value $\sim$1 MHz comparable to the quadrupolar interaction. This strong effect of the pseudodipolar interaction results in well-separated ENDOR transitions, which can be used to monitor nuclear qubits with short selective rf pulses with bandwidths as large as the ENDOR line separation $\approx A^2/\Delta$. Therefore quantum gates with selective pulse length, which can be as short as $\Delta/A^2 \approx 1\mu$s, should be much faster than in liquid NMR, where spin operations are of the order of a few milliseconds or more.[3] Even in the asymmetrical cluster, the weak effect of the pseudodipolar interaction ($\approx 0.05 - 0.1$ MHz) is still much higher than the scalar J coupling or the direct dipolar interaction between nuclei, and thus remains potentially interesting for computational schemes with nuclear spins, as was shown by Mehring and Mende in the case of CaF_2:Ce^{3+}.[9] The effect of the more distant nuclei on nuclear decoherence within a cluster is however, to be investigated, all the more so as the hyperfine couplings with the remote nuclei may again introduce a pseudodipolar interaction between these nuclei and those inside the cluster, which adds to the dipolar and scalar interactions as a possible source of decoherence. The nearest Ga nuclei outside the cluster and identified by ENDOR have hyperfine couplings of about 45–60 MHz for ^{71}Ga (35–47 MHz for ^{69}Ga).[15] From Eq.(3) giving the order of magnitude of the pseudodipolar interaction between inequivalent nuclei and of the corresponding spectral effect and with A_1 and A_2 standing here for the hyperfine coupling constants of a nucleus inside and outside the cluster, respectively, we derive values of the pseudodipolar interaction of about 4–10 kHz. These values are of the same order of magnitude as that of the direct dipolar interaction $\approx$2 kHz, between close nuclei. This means that the pseudodipolar and direct dipolar interactions between nuclei inside and outside the cluster should have similar effects on decoherence.

VI. CONCLUSIONS

To summarize, we studied by ENDOR the nuclear-nuclear interaction mediated by an unpaired electron (pseudodipolar

interaction) in solids, with the prospect of using such interactions in quantum information processing. The system investigated in this paper consists of a linear trimer Ga-Ti^{3+}-Ga in titanium-doped gallium oxide β–Ga_2O_3, in which the unpaired electron spin of titanium interacts equally with the 100% abundant $I = 3/2$ spin of the two gallium nuclei. Taking advantage of the existence of two isotopes, ^{69}Ga (60.1%) and ^{71}Ga (39.9%), this highly symmetrical spin system is ideal for investigating the isotopic effect on the pseudodipolar interaction. We have shown that for the asymmetrical isotopic configuration ^{69}Ga-Ti-^{71}Ga, the nuclear-nuclear interaction mediated by the electron ($\leqslant$0.1 MHz) is weak and smaller than the ENDOR linewidth, thus experimentally unresolved, and scales as $A^3/(g\beta B_0)^2$. The experimental ENDOR spectrum is that of two independent ^{69}Ga and ^{71}Ga nuclei (12 ENDOR lines). On the other hand, for the symmetrical configurations ^{69}Ga-Ti-^{69}Ga and ^{71}Ga-Ti-^{71}Ga, the pseudodipolar interaction has a strong and clearly resolved effect ($\approx$1 MHz), resulting in a multiline (up to 40) ENDOR spectrum, drastically different from the spectrum of the asymmetrical configuration. The strict equivalence of the two nuclei in symmetrical configurations implies that the nuclear eigenstates are either symmetrical or antisymmetrical with respect to the interchange of the nuclei which induces a degeneracy of spin states characterized by opposite parity. The effect of the pseudodipolar interaction, which scales as $A^2/g\beta B_0$, is to lift this degeneracy. These small three-atom clusters combines high spin nuclei, with thus a large qubit register, and strong interactions between nuclei, and nuclear monitoring by an unpaired electron may be potentially interesting for quantum information processing. In such spin systems, nuclear qubits can be monitored with short selective rf and microwave pulses, as shown in a preliminary study.[15]

ACKNOWLEDGMENT

The EPR facility at LCMCP-UMR 7574 is supported by Région Ile-de-France and CNRS.

APPENDIX

The general Hamiltonian for an electron coupled with N nuclei can be written as

$$H = \underbrace{\beta \mathbf{S}\cdot\mathbf{g}\cdot\mathbf{B_0}}_{\mathbf{H}_e} + \underbrace{\sum_{i\leqslant N}(\mathbf{S}\cdot\mathbf{A}_i\cdot\mathbf{I}_i + \mathbf{I}_i\cdot\mathbf{Q}_i\cdot\mathbf{I}_i - g_{n,i}\beta_n\mathbf{I}_i\cdot\mathbf{B}_0)}_{\mathbf{H}_n} \tag{A1}$$

where the sum i runs over the N coupled nuclei. $\mathbf{S}$ and $\mathbf{I}$ stand respectively for the electronic and nuclear spin operators. The eigenstates of $\mathbf{H}_e$ and $\mathbf{H}_n$ are labeled $|S,m_s\rangle$ and $|I_i,m_i\rangle$, respectively. If we consider the case of two inequivalent nuclei coupled with one unpaired electron via isotropic hyperfine interactions, then the previous equation simply reads

$$\begin{aligned} H = {} & \beta \mathbf{S}\cdot \mathrm{g}\cdot \mathrm{B}_0 + \mathbf{S}\cdot(A_1\mathbf{I}_1 + A_2\mathbf{I}_2) + \mathbf{I}_1\cdot\mathbf{Q}_1\cdot\mathbf{I}_1 \\ & + \mathbf{I}_2\cdot\mathbf{Q}_2\cdot\mathbf{I}_2 - \beta_n(g_{n,1}\mathbf{I}_1 + g_{n,2}\mathbf{I}_2)\cdot\mathbf{B}_0. \end{aligned} \tag{A2}$$

In our case, the electron Zeeman Hamiltonian $\mathbf{H_e}$ is of the order of 10 GHz, while the nuclear Hamiltonian $\mathbf{H_n}$ is dominated by the hyperfine interaction with $A_i \approx 100$ MHz. The nuclear Hamiltonian can then be treated as a perturbation of the zeroth-order Hamiltonian $\mathbf{H_e}$. Following Shoemaker's paper,[1] in which the Pryce perturbation method[20] was used, the following effective nuclear Hamiltonian

$$\mathbf{H}'(m_s) = E(m_s) + \mathbf{P}_{m_s}\mathbf{H}_n\mathbf{P}_{m_s} + \sum_{m'_s\neq m_s}\frac{\mathbf{P}_{m_s}\mathbf{H}_n\mathbf{P}_{m'_s}\mathbf{H}_n\mathbf{P}_{m_s}}{E(m'_s) - E(m_s)} \tag{A3}$$

can be derived, where $\mathbf{P}_{m_s}$ represents the projector onto an electron spin m_s manifold. The effective Hamiltonian $\mathbf{H}'(m_s)$ represents a second-order approximation of the exact Hamiltonian $\mathbf{H}$ in an electron spin m_s manifold. The approximate eigenvalues of $\mathbf{H}$ up to second-order are the eigenvalues of the effective Hamiltonian $\mathbf{H}'(m_s)$. The latter can be rewritten as

$$\begin{aligned} \mathbf{H}'(m_s) = {} & g\beta m_s B_0 + m_s(A_1\mathbf{I}_{z,1} + A_2\mathbf{I}_{z,2}) + \frac{m_s}{2g\beta B_0} \\ & \times\left[A_1^2(\mathbf{I}_1^2 - \mathbf{I}_{z,1}^2) + A_2^2(\mathbf{I}_2^2 - \mathbf{I}_{z,2}^2)\right] \\ & + m_s\frac{A_1A_2}{2g\beta B_0}[\mathbf{I}_1^+\mathbf{I}_2^- + \mathbf{I}_1^-\mathbf{I}_2^+] - \frac{1}{4g\beta B_0} \\ & \times\left(A_1^2\mathbf{I}_{z,1} + A_2^2\mathbf{I}_{z,2}\right) + \mathbf{H}_Q + \mathbf{H}_{n\cdot z.}, \end{aligned} \tag{A4}$$

where $\mathbf{H}_Q = \mathbf{I}_1\cdot\mathbf{Q}_1\cdot\mathbf{I}_1 + \mathbf{I}_2\cdot\mathbf{Q}_2\cdot\mathbf{I}_2$ and $\mathbf{H}_{n\cdot z.} = -\beta_n(g_{n,1}\mathbf{I}_1 + g_{n,2}\mathbf{I}_2)\cdot\mathbf{B}_0$. In the above equation, the term:

$$\mathbf{H}_{p.\mathrm{dip.}}(m_s) = m_s\frac{A_1A_2}{2g\beta B_0}\left[\mathbf{I}_1^+\mathbf{I}_2^- + \mathbf{I}_1^-\mathbf{I}_2^+\right] \tag{A5}$$

represents an indirect interaction between the two nuclei mediated by the unpaired electron spin (pseudodipolar interaction).[1] Let us define

$$\mathbf{H}_{h.f.}^{(1)} = m_s\left(A_1\mathbf{I}_{z,1} + A_2\mathbf{I}_{z,2}\right) \tag{A6}$$

$$\begin{aligned} \mathbf{H}_{h.f.}^{(2)} = {} & \frac{m_s}{2g\beta B_0}\left[A_1^2(\mathbf{I}_1^2 - \mathbf{I}_{z,1}^2) + A_2^2(\mathbf{I}_2^2 - \mathbf{I}_{z,2}^2)\right] - \frac{1}{4g\beta B_0} \\ & \times\left(A_1^2\mathbf{I}_{z,1} + A_2^2\mathbf{I}_{z,2}\right) + m_s\frac{A_1A_2}{2g\beta B_0}[\mathbf{I}_1^+\mathbf{I}_2^- + \mathbf{I}_1^-\mathbf{I}_2^+]. \end{aligned} \tag{A7}$$

In our case, we have the following orders of magnitude: $\mathbf{H}_{h.f.}^{(1)} \sim A_i \approx 100$ MHz, $\mathbf{H}_{h.f.}^{(2)} \sim A_i^2/g\beta B_0 \approx 1$ MHz (with $g\beta B_0 \approx 9500$ MHz) and $\mathbf{H}_Q \approx \mathbf{H}_{n.z.} \approx 1$ MHz. Therefore $\mathbf{H}_{h.f.}^{(2)} + \mathbf{H}_Q + \mathbf{H}_{n.z.}$ can be treated as a perturbation with respect to $\mathbf{H}_{h.f.}^{(1)}$.

1. Case of inequivalent nuclei

In this case, the zeroth-order basis is made of the eigenstates $|S,m_s\rangle|I_1,m_1,I_2,m_2\rangle \equiv |m_s\rangle|m_1,m_2\rangle$ of $\mathbf{H}_{h.f.}^{(1)}$. Since $A_1 \neq A_2$ (inequivalent nuclei), these states are not degenerate and first-order approximations of the eigenvalues of $\mathbf{H}'(m_s)$ are directly given by the diagonal elements of $\mathbf{H}'(m_s)$ in the above basis. Thus the approximate eigenvalues are the sum of the following

terms:

$$E^{(0)}(m_s,m_1,m_2) = g\beta B_0 m_S + m_S(A_1 m_1 + A_2 m_2), \quad \text{(A8)}$$

$$E^{(1)}_{n.z.,Q}(m_s,m_1,m_2) = -\beta_n B_0(g_{n,1}m_1 + g_{n,2}m_2) + \frac{1}{2}Q_1\left[3m_1^2 - I_1(I_1+1)\right] + \frac{1}{2}Q_2 \times \left[3m_2^2 - I_2(I_2+1)\right] \quad \text{(A9)}$$

$$E^{(1)}_{h.f.}(m_s,m_1,m_2) = \frac{A_1^2}{2g\beta B_0}m_s\left[I_1(I_1+1) - m_1^2\right] + \frac{A_2^2}{2g\beta B_0}m_s\left[I_2(I_2+1) - m_2^2\right] - \frac{1}{4g\beta B_0}\left(A_1^2 m_1 + A_2^2 m_2\right). \quad \text{(A10)}$$

In the above equations, we considered axial quadrupolar tensors and Q_i ($i = 1,2$) stands for the effective component of tensor $\mathbf{Q}_i$ along the magnetic field direction. The terms $E^{(1)}_{n.z.,Q}$ and $E^{(1)}_{h.f.}$ represent the first-order contributions of $\mathbf{H}_Q + \mathbf{H}_{n.z.}$ and $\mathbf{H}^{(2)}_{h.f.}$, respectively, to the eigenvalues of $\mathbf{H}'(m_s)$, and consequently second-order corrections with respect to the exact Hamiltonian $\mathbf{H}$. It must be noticed that, in the case of inequivalent nuclei, the pseudodipolar term does not give first-order corrections to $\mathbf{H}'(m_s)$ since it has only off-diagonal elements. The pseudodipolar interaction contributes to only second-order corrections to $\mathbf{H}'(m_s)$, which are given by

$$\begin{aligned} &E^{(2)}(m_s,m_1,m_2) \\ &= \frac{|\langle m_1,m_2|\mathbf{H}_{p.\mathrm{dip.}}(m_s)|m_1-1,m_2+1\rangle|^2}{E^{(0)}(m_s,m_1,m_2) - E^{(0)}(m_s,m_1-1,m_2+1)} \\ &\quad + \frac{|\langle m_1,m_2|\mathbf{H}_{p.\mathrm{dip.}}(m_s)|m_1+1,m_2-1\rangle|^2}{E^{(0)}(m_s,m_1,m_2) - E^{(0)}(m_s,m_1+1,m_2-1)} \\ &= 2\left(\frac{m_s A_1 A_2}{2g\beta B_0}\right)^2 \\ &\quad \times \frac{m_1\left[I_2(I_2+1) - m_2^2\right] - m_2\left[I_1(I_1+1) - m_1^2\right]}{m_s(A_1 - A_2)}, \end{aligned} \quad \text{(A11)}$$

These corrections actually represent third-order corrections to the exact Hamiltonian $\mathbf{H}$ for they scale as $A^3/(g\beta B_0)^2$. The ENDOR selection rules are $\Delta m_s = 0, \Delta m_1 = \pm 1, \Delta m_2 = 0$ or $\Delta m_s = 0, \Delta m_1 = 0$, and $\Delta m_2 = \pm 1$. For a transition $|m_1,m_2\rangle \leftrightarrow |m_1+1,m_2\rangle$ on nucleus 1, the ENDOR frequency is thus

$$\nu = \left| m_s A_1 - \frac{m_s A_1^2(2m_1+1)}{2g\beta B_0} - \frac{A_1^2}{4g\beta B_0} - \beta_n B_0 g_{n,1} + \frac{3}{2}Q_1(2m_1+1) + 2m_s\left(\frac{A_1 A_2}{2g\beta B_0}\right)^2 \times \frac{I_2(I_2+1) - m_2^2 + 2m_1 m_2 + m_2}{A_1 - A_2}\right|. \quad \text{(A12)}$$

First ignoring the last term due to the pseudodipolar interaction in the above equation, we thus expect $2I_1 \times (2S+1)$ (=6 for $I_1 = 3/2$ and $S = 1/2$) ENDOR lines for nucleus 1. Each transition actually has a degeneracy corresponding to the $2I_2 + 1$ possible values of the spin state m_2 of nucleus 2. If we now take into account the last term in the above expression, which represents the effect of the coupling between nuclei 1 and 2 through the pseudodipolar interaction, we see that the ENDOR transitions on nucleus 1 now depend on the spin state m_2 of nucleus 2 through the last term. This gives rise to a splitting of each ENDOR transition $\Delta m_1 = \pm 1$ on nucleus 1, since now an ENDOR frequency for nucleus 1 depends on the spin state of nucleus 2. These splittings are small, of the order of $(A_1 A_2/g\beta B_0)^2/(A_1 - A_2) \approx 0.06$ MHz (for $A_1 \approx 128$ MHz and $A_2 \approx 100$ MHz). We can, however, notice that the effect of the pseudodipolar coupling is significantly enhanced when $A_1 \approx A_2$ owing to the $1/(A_1 - A_2)$ factor, so that an exceptional effect can be expected in the case of equivalent nuclei. One should also be aware that the degeneracy of a $\Delta m_1 = \pm 1$ ENDOR transition may not be fully lifted by the pseudodipolar interaction. As can be seen from the above equation, ENDOR transitions corresponding to two spin states m_2 and m_2' of nucleus 2 satisfying $m_2 + m_2' = 2m_1 + 1$ will occur at the same frequency. In the case $I_1 = I_2 = 3/2$, degeneracy thus remains when $\{m_2,m_2'\} = \{-1/2,-3/2\}$ for the $-3/2 \leftrightarrow -1/2$ transition, $\{m_2,m_2'\} = \{-1/2,1/2\}$ or $\{-3/2,3/2\}$ for the $-1/2 \leftrightarrow 1/2$ transition and $\{m_2,m_2'\} = \{1/2,3/2\}$ for the $1/2 \leftrightarrow 3/2$ transition on nucleus 1, so that each ENDOR line should be split into at most two or three sublines due to the pseudodipolar interaction. In the case $I_2 = 1/2$, no splitting but only a small shift by $m_s(A_1 A_2/g\beta B_0)^2/(A_1 - A_2)$ of the $-1/2 \leftrightarrow 1/2$ transition occurs.

2. Case of equivalent nuclei

When the nuclei correspond to the same isotope ($I_1 = I_2 = I$) and are magnetically equivalent ($A_1 = A_2 = A$ and $Q_1 = Q_2 = Q$), the pseudodipolar term will produce first-order corrections to the effective Hamiltonian $\mathbf{H}'(m_s)$ (thus second-order corrections to the exact Hamiltonian $\mathbf{H}$). Since the magnetic field $\mathbf{B_0}$ is a pseudo-vector, Hamiltonian Eq. (A1) is invariant under the interchange of the two nuclei. The nuclear eigenstates must then be either symmetrical or antisymmetrical with respect to the interchange of the nuclei, so that suitable zeroth-order eigenstates are

$$|I,m_1,m_2,\mathcal{P}\rangle = \frac{1}{\sqrt{2}}(|I_1 = I,m_1,I_2 = I,m_2\rangle + \mathcal{P}|I_2 = I,m_2,I_1 = I,m_1\rangle), \quad \text{(A13)}$$

where $\mathcal{P} = \pm 1$ is the parity of the eigenstate of Hamiltonian Eq. (A2).[1,2] Ignoring the pseudodipolar interaction, states with fixed values of m_1 and m_2 but opposite values of $\mathcal{P}$ are degenerate. As a first-order effect with respect to $\mathbf{H}'(m_s)$, the pseudodipolar interaction lifts this two fold degeneracy in the case where $m_1 = m_2 \pm 1$, as shown in Fig. 6. This term also leads to a mixing of states of same value of $M = m_1 + m_2$ and yields additional second-order energy shifts, which are not considered here.[2] The first-order approximations of the eigenvalues of $\mathbf{H}'(m_s)$ are given by

$$E^{(0)}(m_s,m_1,m_2,\mathcal{P}) = g\beta B_0 m_S + A m_s(m_1 + m_2), \quad \text{(A14)}$$

$$E^{(1)}_{n.z.,Q}(m_s,m_1,m_2,\mathcal{P}) = -g_n\beta_n B_0(m_1 + m_2) + \tfrac{3}{2}Q\left[m_1^2 + m_2^2 - \tfrac{2}{3}I(I+1)\right] \quad \text{(A15)}$$

$$E^{(1)}_{h.f.}(m_s,m_1,m_2,\mathcal{P}) = \frac{A^2}{2g\beta B_0} m_s\left[2I(I+1)-\left(m_1^2+m_2^2\right)\right] - \frac{A^2}{4g\beta B_0} \times (m_1+m_2) + \mathcal{P}\frac{A^2}{2g\beta B_0} m_s[I(I+1)-m_1m_2] \times [\delta(m_1,m_2-1)+\delta(m_1,m_2+1)] \quad \text{(A16)}$$

where δ stands for the classical Kronecker distribution. The difference with the case of inequivalent nuclei is the occurrence of the last term in the expression of $E^{(1)}_{h.f.}$ due to the pseudodipolar interaction. The ENDOR selection rules are $\Delta m_s = 0, \Delta m_1 = \pm 1, \Delta m_2 = 0, \Delta\mathcal{P} = 0$ or $\Delta m_s = 0, \Delta m_1 = 0, \Delta m_2 \pm 1, \Delta\mathcal{P} = 0$. The frequencies for $m_1 \leftrightarrow m_1 + 1$ transitions of nucleus 1 are thus given by

$$\nu = \Big| m_s A - g_n\beta_n B_0 + (2m_1+1)\left(\frac{3}{2}Q - \frac{m_s A^2}{2g\beta B_0}\right) - \frac{A^2}{4g\beta B_0} + m_s P\frac{A^2}{2g\beta B_0}\{[I(I+1)-(m_1+1)m_2] \times [\delta(m_1+1,m_2-1)+\delta(m_1+1,m_2+1)] - [I(I+1)-m_1m_2][\delta(m_1,m_2-1) + \delta(m_1,m_2+1)]\}\Big|. \quad \text{(A17)}$$

The effect of the pseudodipolar interaction on the ENDOR frequencies is now of the order of $A^2/g\beta B_0 \approx 1$ MHz, thus yielding much larger splittings of the nuclear energy levels than in the case of inequivalent nuclei.

*laurent-binet@chimie-paristech.fr

[1] D. Schoemaker, Phys. Rev. **174**, 1060 (1968).
[2] T. Feuchtwang, Phys. Rev. **126**, 1628 (1962).
[3] N. A. Gershenfeld and I. L. Chuang, Science **275**, 350 (1997).
[4] D. Cory *et al.*, Fortschr. Phys. **48**, 875 (2000).
[5] L. M. K. Vandersypen and I. L. Chuang, Rev. Mod. Phys. **76**, 1037 (2005).
[6] I. Chuang, N. Gershenfeld, M. Kubinec, and D. Leung, Proc. R. Soc. London Ser. A **454**, 447 (1998).
[7] M. Mehring, J. Mende, and W. Scherer, Phys. Rev. Lett. **90**, 153001 (2003).
[8] B. E. Kane, Nature **393**, 133 (1998).
[9] M. Mehring and J. Mende, Phys. Rev. A **73**, 52303 (2006).
[10] N. Khaneja, Phys. Rev. A **76**, 32326 (2007).
[11] J. S. Hodges, J. C. Yang, C. Ramanathan, and D. G. Cory, Phys. Rev. A **78**, 10303 (2008).
[12] E. Aubay and D. Gourier, J. Phys. Chem. **96**, 5513 (1992).
[13] E. Aubay and D. Gourier, Phys. Rev. B **47**, 15023 (1993).
[14] L. Binet and D. Gourier, J. Phys. Chem. **100**, 17630 (1996).
[15] F. Mentink-Vigier, L. Binet, G. Vignoles, D. Gourier, and H. Vezin, Phys. Rev. B **82**, 184414 (2010).
[16] N. Ramsey, Phys. Rev. **91**, 303 (1953).
[17] G. Feher, Phys. Rev. **105**, 1122 (1957).
[18] R. Barklie, J. Niklas, and J. Spaeth, J. Phys. C: Solid State Physics **13**, 1757 (1980).
[19] J. Hage, J. Niklas, and J. Spaeth, Mater. Sci. Forum **10–12**, 259 (1986).
[20] M. Pryce, Proc. Phys. Soc. London, Sect. A **63**, 25 (1950).
[21] A. Saurat and R. Revcolevcschi, Rev. Int. Hautes Temp. Réfract. **8**, 291 (1971).
[22] S. Stoll and A. Schweiger, J. Magn. Reson. **178**, 42 (2006).
[23] M. Iwasaki, J. Magn. Reson. **16**, 417 (1974).
[24] J. Spaeth and H. Overhof, *Point Defects in Semiconductors and Insulators* (Springer, Berlin, 2003).
[25] G. Feher, Phys. Rev. **103**, 834 (1956).
[26] A. Abragam and B. Bleaney, *Electron Paramagnetic Resonance of transition ions* (Clarendon Press Oxford, 1970).
[27] W. Warren, N. Gershenfeld, and I. Chuang, Science **277**, 1688 (2010).
[28] S. L. Braunstein, C. M. Caves, R. Jozsa, N. Linden, S. Popescu, and R. Schack, Phys. Rev. Lett. **83**, 1054 (1999).
[29] P. O. Boykin, T. Mor, V. Roychowdhury, F. Vatan, and R. Vrijen, Proc. Nat. Acad. Sci. USA **99**, 3388 (2002).
[30] A. Kessel' and V. Ermakov, JETP Lett. **70**, 61 (1999).
[31] A. K. Khitrin and B. M. Fung, J. Chem. Phys. **112**, 6963 (2000).
[32] N. Sinha, T. S. Mahesh, K. V. Ramanathan, and A. Kumar, J. Chem. Phys. **114**, 4415 (2001).
[33] H. Kampermann and W. S. Veeman, J. Chem. Phys. **122**, 214108 (2005).
[34] C. Yannoni, M. Sherwood, D. Miller, I. Chuang, L. Vandersypen, and M. Kubinec, Appl. Phys. Lett. **75**, 3563 (1999).